Therapeutic antitumor immunity by checkpoint blockade is enhanced by ibrutinib, an inhibitor of both BTK and ITK

Idit Sagiv-Barfi[a], Holbrook E. K. Kohrt[a], Debra K. Czerwinski[a], Patrick P. Ng[b], Betty Y. Chang[b], and Ronald Levy[a,1]

[a]Division of Oncology, Department of Medicine, Stanford University, Stanford, CA 94305-5151; and [b]Department of Research, Pharmacyclics, Inc., Sunnyvale, CA 94085-4521

Contributed by Ronald Levy, January 14, 2015 (sent for review November 11, 2014; reviewed by Jan A. Burger and Antoni Ribas)

Monoclonal antibodies can block cellular interactions that negatively regulate T-cell immune responses, such as CD80/CTLA-4 and PD-1/PD1-L, amplifying preexisting immunity and thereby evoking antitumor immune responses. Ibrutinib, an approved therapy for B-cell malignancies, is a covalent inhibitor of BTK, a member of the B-cell receptor (BCR) signaling pathway, which is critical to the survival of malignant B cells. Interestingly this drug also inhibits ITK, an essential enzyme in Th2 T cells and by doing so it can shift the balance between Th1 and Th2 T cells and potentially enhance antitumor immune responses. Here we report that the combination of anti–PD-L1 antibody and ibrutinib suppresses tumor growth in mouse models of lymphoma that are intrinsically insensitive to ibrutinib. The combined effect of these two agents was also documented for models of solid tumors, such as triple negative breast cancer and colon cancer. The enhanced therapeutic activity of PD-L1 blockade by ibrutinib was accompanied by enhanced antitumor T-cell immune responses. These preclinical results suggest that the combination of PD1/PD1-L blockade and ibrutinib should be tested in the clinic for the therapy not only of lymphoma but also in other hematologic malignancies and solid tumors that do not even express BTK.

ibrutinib | PD-1/PD-L1 blockade | lymphoma | solid tumors

One of the most exciting recent developments in cancer therapy has been the introduction of immune checkpoint blockade. Immune checkpoints include negative regulators that function normally to protect against autoimmunity (1). However, these same checkpoints can also dampen the host immune response to novel antigens created by somatic mutations in tumor cells. Ipilimumab, a monoclonal antibody (mAb) targeting CTLA-4 (cytotoxic T-lymphocyte-associated protein 4), a negative signal transducer on T cells, was the first checkpoint-blocking antibody to be approved by the US FDA for the treatment of cancer. This original approval was limited to unresectable or metastatic melanoma (2). More recently, Pembrolizumab, a second checkpoint-blocking antibody, was also approved for advanced melanoma (3). This antibody targets the Programmed Death 1 (PD-1; CD279) molecule. PD-1, expressed on T cells, B cells, and other immune effector cells (4) interacts with the PD-1 ligand (PD-L1; B7-H1; CD274) expressed on a wide variety of tumors (5–8), resulting in a negative signal to the T cell. Clinical trials with mAbs targeting either PD-1 or PD-L1 have shown dramatic responses and long-term regressions in patients with melanoma, renal carcinoma, nonsmall cell lung cancer, Hodgkin's Lymphoma, and other cancers (9–12). However, dramatic as they are, these remissions occur in a minority of the patients. A number of strategies are being developed to enhance the therapeutic effects of PD1/PD-L1 blockade, such as combining it with other anticancer therapies (13–15).

A parallel advance in cancer therapy has been the development of small molecule drugs that target critical survival pathways in cancer cells. Many of these are tyrosine kinase inhibitors, Gleevec being the prototype. One recent member of this class is ibrutinib, a covalent inhibitor of BTK (Bruton's tyrosine kinase) (16), a key enzyme in the B-cell receptor signaling pathway and a very effective therapy for chronic lymphocytic leukemia (CLL) Mantle cell lymphoma (MCL) and Waldenstrom's Macroglobulinemia (17, 18). This drug also inhibits other tyrosine kinases (16), including ITK (interleukin-2-inducible T-cell kinase), an enzyme important for the survival of Th2 T cells (19), and therefore ibrutinib might have immunomodulatory effects in addition to direct anti-lymphoma effects.

We now have the opportunity to combine targeted therapies with immune checkpoint blockade. In particular, we combined ibrutinib with an anti–PD-L1 antibody and treated tumors that have no intrinsic sensitivity to ibrutinib.

Results

A20, a Lymphoma That Is Insensitive to Ibrutinib. To test the indirect immunomodulatory effects of ibrutinib, we first sought lymphoid malignancies that had no dependence on BTK and were insensitive to the direct effects of ibrutinib. For instance, A20, a mature B-cell lymphoma of BALB/c mice is insensitive to ibrutinib in vitro (IC50 > 10 μM; Fig. 1*A*) although BTK is expressed by these cells (Fig. S1). By comparison, H11 a different malignant lymphoid line was sensitive to ibrutinib in vitro (IC50 ~ 0.5 μM). Moreover, ibrutinib did not impede the growth of A20 in syngeneic animals (Fig. 1 *B* and *C*) nor did it have any effect on the survival of tumor-bearing animals (Fig. 1*B*), even at doses that fully occupied BTK in the normal splenic B cells (Fig. S2). This dose and schedule of ibrutinib also resulted in

Significance

Antibodies that block the negative signals between PD1-Ligand on tumor cells and PD-1 on T cells are effective therapies against several types of cancer. Ibrutinib, a covalent inhibitor of BTK is an approved therapy for B-cell leukemia and lymphoma. But ibrutinib also inactivates ITK, an enzyme required for certain subsets of T lymphocytes (Th2 T cells). We found that the combination of anti–PD-L1 antibodies and ibrutinib led to impressive therapeutic effects not only in animal models of lymphoma but, surprisingly, also in models of breast cancer and colon cancer. Based on these preclinical results, we suggest that the combination of PD-1/PD-L1 blockade and ibrutinib be tested broadly in patients with lymphoma and also in other hematologic malignancies and solid tumors.

Author contributions: I.S.-B., H.E.K.K., B.Y.C., and R.L. designed research; I.S.-B., D.K.C., and P.P.N. performed research; I.S.-B., D.K.C., P.P.N., B.Y.C., and R.L. analyzed data; and I.S.-B., H.E.K.K., P.P.N., and R.L. wrote the paper.

Reviewers: J.A.B., The University of Texas MD Anderson Cancer Center; and A.R., Ronald Reagan UCLA Medical Center.

The authors declare no conflict of interest.

[1]To whom correspondence should be addressed. Email: levy@stanford.edu.

This article contains supporting information online at www.pnas.org/lookup/suppl/doi:10.1073/pnas.1500712112/-/DCSupplemental.

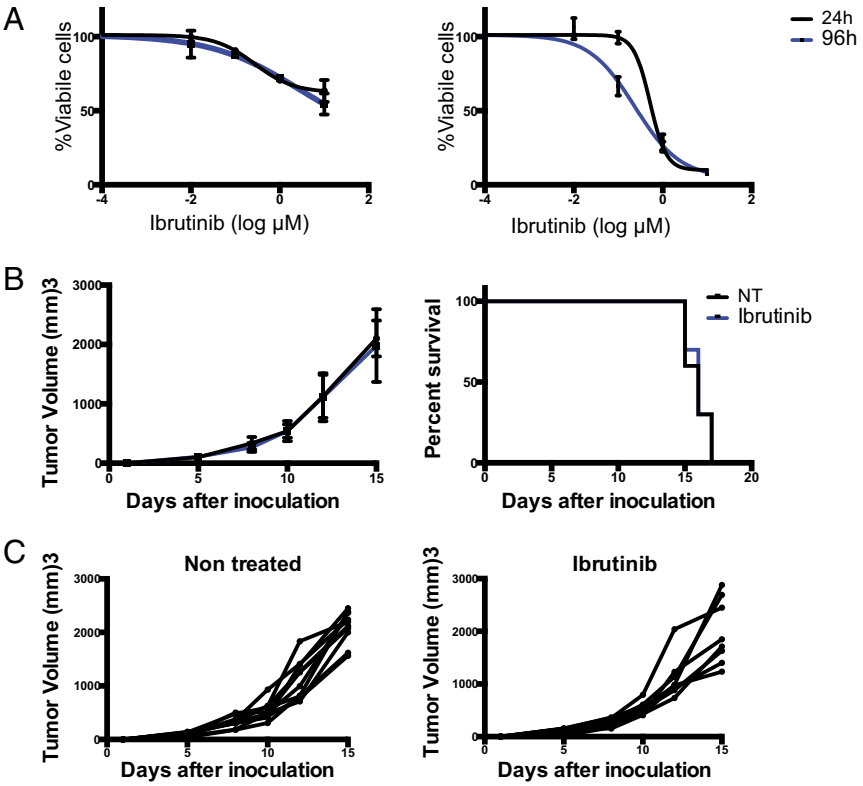

Fig. 1. A20 cell line is insensitive to ibrutinib in vitro and in vivo. (*A*) Cell survival as measured by presto blue. Cells were incubated with serial dilutions of ibrutinib at concentration ranging form 0.04–10 μM or with media alone for the indicated time. (*Left*) A20 cells. (*Right*) H11 cells. (*B*) Tumor growth curves (*Left*) and Kaplan–Meier survival plots of the treated mice (*Right*). (*C*) Individual mice tumor growth curves.

occupancy of ITK in thymic T cells and inhibited the autophosphorylation of ITK and its activity in phosphorylation of downstream kinases (Fig. S3).

Ibrutinib in Combination with Anti–PD-L1 Can Cure Established A20 Tumors. A20 lymphoma cells express high levels of PD-L1 (Fig. 2*A*). However, the antibody against PD-L1 had no direct effect on the growth of A20 cells in vitro (Fig. S4*A*). Treatment of animals with established tumors by anti–PD-L1 antibody resulted in delayed tumor growth and a modest increase in overall survival (Fig. 2 *B*, *C*, and *F*). However, anti–PD-L1 antibody was not curative in any of the mice. Interestingly, the tumor responses to anti–PD-L1 therapy were dichotomous, with one subgroup of mice responding and another group of mice showing no antitumor effect. These observations were confirmed in three separate experiments.

Depletion of CD4 and CD8 T cells during the treatment period abrogated the antitumor effect of anti–PD-L1 antibody, confirming the role of T cells in its mechanism of action (Fig. 2*D*).

In contrast, the addition of ibrutinib to anti–PD-L1 resulted in the cure of approximately half of the mice, and a delay of tumor growth and prolongation of survival in the remaining mice (Fig. 2 *C* and *F*). Ibrutinib administration did not affect tumor PD-L1 expression level (Fig. S5). These results were consistent in multiple replicate experiments.

We found evidence of tumor specific T cells in the mice treated by the combination of ibrutinib and anti–PD-L1 antibody. Splenic T cells from these mice produced IFN-γ upon exposure to the irradiated A20 tumor cells in vitro, but not after exposure to an unrelated BALB/c lymphoma. Interestingly, we found no evidence by this assay of antitumor T cells in mice treated either with ibrutinib, alone or with anti–PD-L1 antibody, alone (Fig. 2 *E* and *G*). The IFN-γ producing T cells were of the CD44-high population, a marker for central memory T cells.

Therefore, ibrutinib was able to convert a weak antitumor T-cell immune response induced by anti–PD-L1 antibody into a powerful one, in this lymphoma model that was insensitive to ibrutinib as a single therapy. We confirmed this combined therapeutic effect in a second lymphoid malignancy, the J558 myeloma tumor, which is also insensitive to ibrutinib as a single agent (Fig. S6).

The Combination of Ibrutinib and Anti–PD-L1 Inhibits the Growth of Solid Tumors. Because ibrutinib enhanced the antitumor T-cell response induced by anti–PD-L1 therapy against lymphoma tumors that had no intrinsic sensitivity to ibrutinib, we wondered whether ibrutinib might also enhance such immune responses against solid tumors. Therefore, we evaluated this therapy combination in tumors that do not even express BTK (Fig. S1). 4T1 is a triple negative breast cancer, and CT26 is a colon cancer.

4T1 cells express low levels of PD-L1 (Fig. 3*A*). As expected, neither ibrutinib nor anti–PD-L1 had any effect on the survival of these cells in vitro (Fig. S4 *A* and *B*). We injected luciferase-transduced 4T1 cells (4T1-Luc) into the mammary fat pads of syngeneic BALB/c mice and treated the established tumors with ibrutinib alone or anti–PD-L1 alone (Fig. 3*B*). We observed neither a delay in primary tumor growth nor an increase in animal survival (Fig. 3 *C*, *D*, and *G*). In contrast, the combination of ibrutinib and anti–PD-L1 resulted in reduced size of primary tumors, increased survival and fewer lung metastases (Fig. 3 *D*, *E*, and *H*). In concordance with the results seen in the A20 lymphoma tumor model, the combination therapy generated specific antitumor T cells (Fig. 3 *F* and *I*).

Myeloid-derived suppressor cells (MDSCs) are known to be massively increased and are presumed to play an important role in the growth and metastasis of this 4T1 tumor model. However, the combined therapy with ibrutinib and anti–PD-L1 antibody had no effect on the number or proportion of the elevated circulating or splenic MDSC (Fig. S7).

CT26 colon cancer cells express low levels of PD-L1 (Fig. 4*A*). Similar to the observations in the previous models, there was no effect of either ibrutinib or of anti–PD-L1 antibody on the

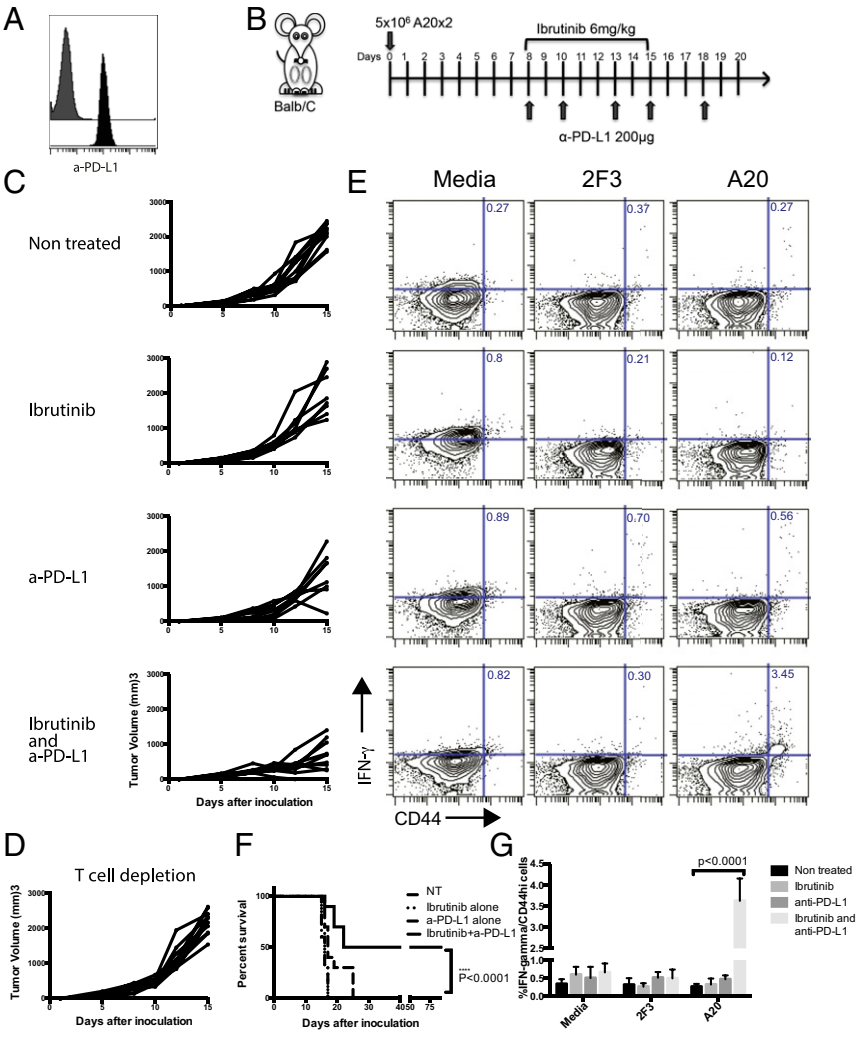

Fig. 2. Ibrutinib in combination with anti–PD-L1 induces an antitumor immune response. (*A*) PD-L1 expression of A20 in comparison with rat IgG2a isotype control. (*B*) Treatment schema. BALB/c mice were inoculated with 5×10^6 A20 cells s.c. on both right and left of their abdomen, and tumor growth was monitored with a digital caliper. Ibrutinib (6 mg/kg) was IP injected daily for 8 d. Starting day 8, anti–PD-L1 (200 μg) was IP injected for a total of five doses, three times a week starting on day 8. (*C*) Tumor growth curves (n = 10 mice per group): nontreated:ibrutinib, not significant; nontreated:anti–PD-L1, P = 0.0038; nontreated:ibrutinib and anti–PD-L1, $P < 0.0001$. (*D*) Tumor growth curves of CD4/CD8 depleted mice. a-CD4/CD8 depleting antibodies (0.5 and 0.1 mg, respectively) were IP injected on days 6–8, 12, and 15 (n = 10 mice per group). (*E*) Intracellular IFN-γ production of CD8+ cells. On day 7 posttreatment, splenocytes were cocultured with either media or 1×10^6 irradiated 2F3 or A20 cells for 24 h and in the presence of monensin for the last 6 h. Intracellular IFN-γ was assayed, and results were gated on CD3+ cells; indicated are the proportion of IFN-γ+ cells as a percentage of CD44hi cells. (*F*) Kaplan–Meier survival plots of the treated mice. (*G*) Percentage of IFN-γ+ CD8+ cells of splenocytes incubated with Media, irradiated 2F3 or A20 cells (n = 6 mice per group).

growth in vitro of the CT26 tumor cells (Fig. S4 *A* and *C*). Therapy with anti–PD-L1 antibody showed modest antitumor effects, and once again, as with the other tumor models, only a subset of the mice responded to this treatment. The addition of ibrutinib to anti–PD-L1 resulted in an increase in the number of the responding mice and was able to cure ∼30% of the mice (Fig. 4 *C* and *G*). These results were typical of four independent experiments. Once again, we were able to demonstrate tumor-specific T cells in the blood and spleen of the CT26-bearing animals that were treated with the combined ibrutinib and anti–PD-L1 antibody (Fig. 4*D*). CT26 expresses a tumor-specific antigen, AH1 [corresponding to amino acids 423–431 of the endogenous murine leukemia virus (MuLV), gp90 gene] (20). We used an MHC tetramer to detect AH1-specific CD8 T cells in these treated mice. We found specific tetramer-binding CD8 cells in the mice treated and cured by the combined ibrutinib and anti–PD-L1 treatment (Fig. 4 *E* and *H*).

We next tested whether mice cured with this combined therapy developed long-term immune memory. We rechallenged the mice that had rejected the CT26 tumor either with the same CT26 tumor cells or with the unrelated 4T1 tumor. These rechallenged mice were resistant to the CT26 tumor but not to the unrelated 4T1 tumor (Fig. 5). This result indicates that the mice cured by the combined therapy had long-term memory to tumor antigens expressed specifically in the CT26 tumor.

Discussion

Small molecule targeted therapies and immune checkpoint blocking antibodies are among the most exciting new cancer treatments. Here we combined ibrutinib, a covalent BTK inhibitor, with an anti–PD-L1 monoclonal antibody and tested the combination in a series of preclinical animal models.

This combination led to a remarkable therapeutic outcome, not by their effects on the tumor cells directly, but rather by their effects on the immune system.

To date, multiple combinations using immunotherapy and small molecules are being explored in both preclinical and clinical settings. Clinical trials are on-going combining ibrutinib with monoclonal anti-CD20 antibodies in the treatment of non-hodgkin's lymphoma (NCT01569750), including follicular lymphoma (NCT01980654), mantle cell lymphoma (NCT01880567), and nongerminal center B-cell subtype of DLBCL (NCT01569750). Ibrutinib is being studied in CLL in combination with rituximab (NCT02007044) and lenalinomide (NCT02200848, NCT02160015, NCT01886859). In these studies, ibrutinib is used to target the cancer-associated kinase. The immune modulating property of ibrutinib in targeting the T-cell associated kinase, ITK, introduces a strong rationale to combine this drug with other immune modulating therapies such as checkpoint blockade agents. Combination therapy with PD1 blockade and anti-CTLA4, ipilimumab, showed additive activity to effects of either agent alone in advanced melanoma (13). This combination is currently being explored in other

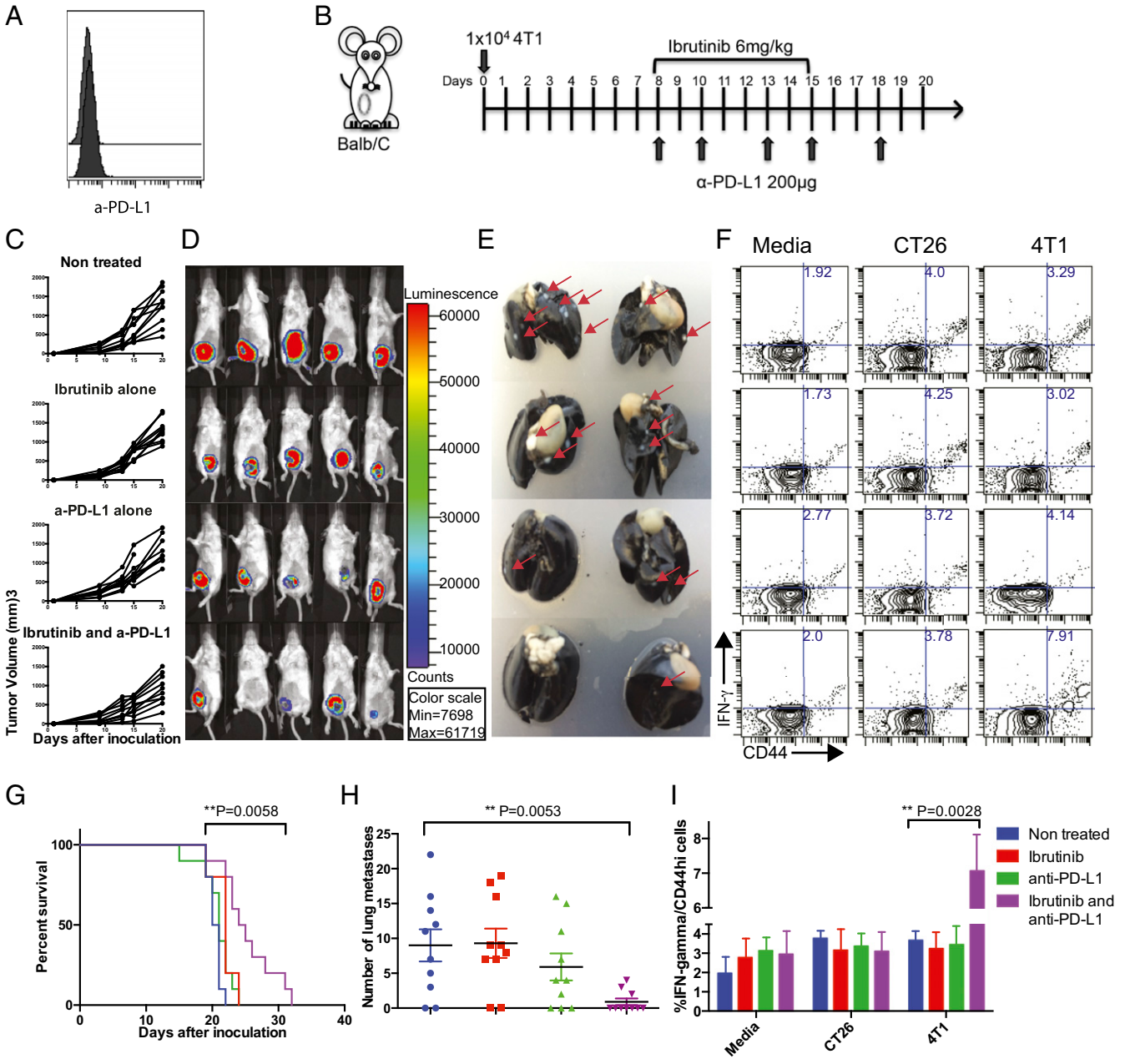

Fig. 3. The combination of ibrutinib with anti–PD-L1 reduces tumor burden in 4T1 tumor-bearing mice. (*A*) PD-L1 expression of 4T1-Luc cells in comparison with rat IgG2a isotype control. (*B*) Treatment schema. Six- to 8-week-old BALB/c mice were inoculated with 0.01×10^6 4T1-Luc cells s.c. into the right side of their abdomen; ibrutinib and anti–PD-L1 antibody were i.p. injected. (*C*) Tumor growth curves as measured with a digital caliper ($n = 10$ mice per group); nontreated:ibrutinib, not significant; nontreated:anti–PD-L1, not significant; nontreated:ibrutinib and anti–PD-L1, not significant. (*D*) Mice bioluminescence on day 21 postinoculation. (*E*) On day 21 after tumor inoculation, lungs were inflated with India ink, and surface metastases appeared as white nodules at the surface of black lungs and were counted under a microscope ($n = 10$ mice per group). (*F*) Antitumor T-cell responses: Intracellular IFN-γ production of CD8+ cells. Results were gated on CD3+ cells; indicated are the proportion of IFN-γ+ cells as a percentage of CD44hi cells ($n = 10$ mice per group). (*G*) Kaplan–Meier survival plots of the treated mice ($n = 10$ mice per group). (*H*) Lung metastasis on day 21 after tumor inoculation ($n = 10$ mice per group). (*I*) Percentage of IFN-γ+ CD8+ cells of splenocytes incubated with Media, irradiated CT26 or 4T1-Luc cells ($n = 6$ mice per group).

solid tumor types (NCT02304458, NCT02210117). PD1 blockade and anti-CTLA4 therapy was associated with significant grade 3 and 4 toxicities similar to the toxicity profile of anti-CTLA4 alone. An important clinical experiment combined the BRAF inhibitor, vemurafenib, with ipilimumab in the treatment of melanoma. This combination suffered from excessive toxicity, particularly in the liver (21). This experience serves as a warning when combining new agents. Both ibrutinib and PD1 blocking antibodies have been well tolerated as single agents; however, the dosing, timing, and sequencing of treatment must be considered when planning clinical trials.

Ibrutinib has to date been thought of as an inhibitor of a survival pathway intrinsic to lymphoid cells and it is used exclusively in BTK-expressing lymphoid malignancies. We chose mouse tumor models that share over 90% sequence identity to human ITK and BTK proteins, including the conserved cys residue at the ATP binding pocket. These tumors have no dependence on BTK, and we evaluated whether ibrutinib could, in addition, work by

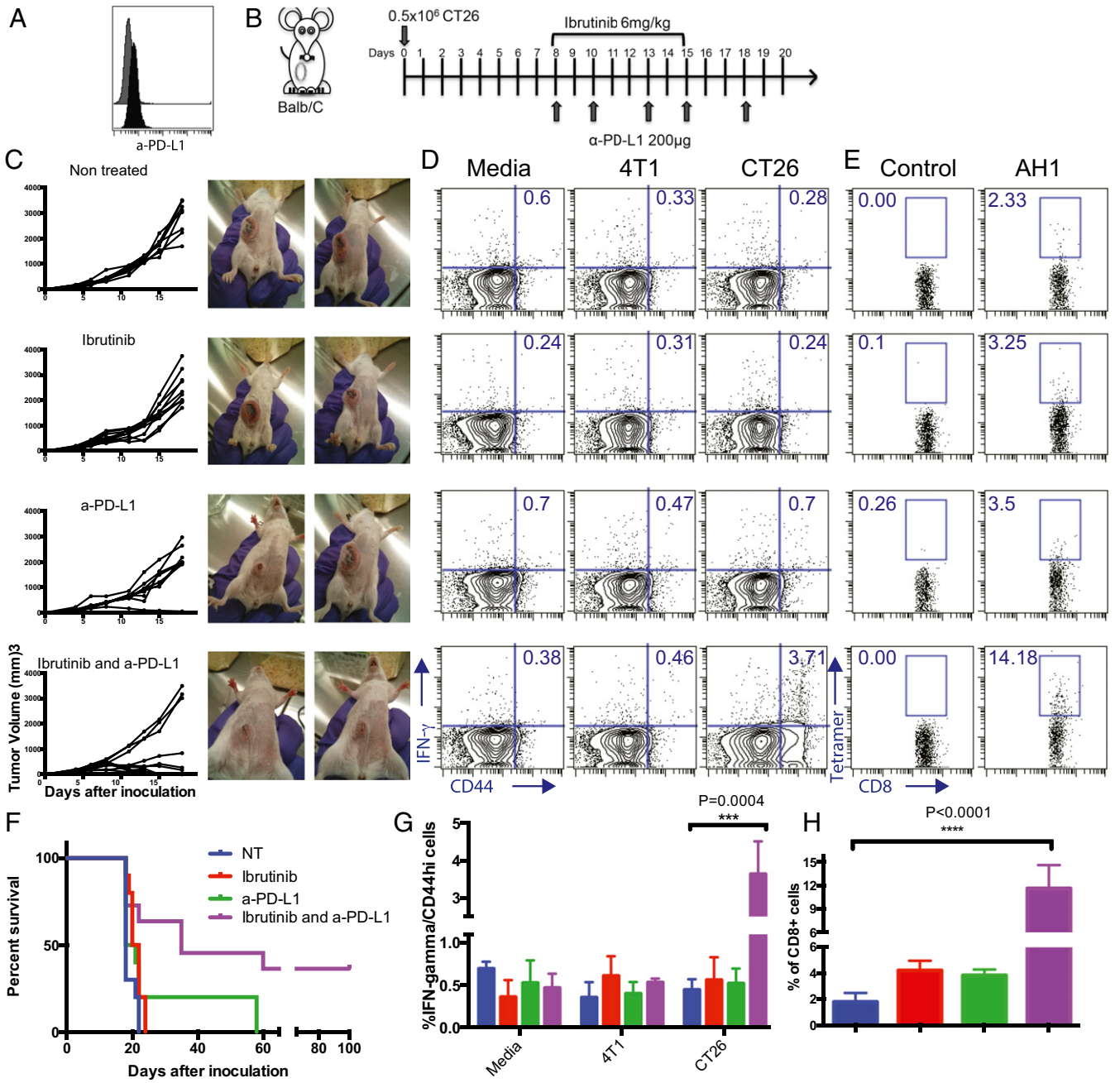

Fig. 4. The combination of ibrutinib with anti–PD-L1 improves survival and cures CT26 tumor bearing mice. (*A*) PD-L1 expression of CT26 in comparison with rat IgG2a isotype control. (*B*) Treatment schema- BALB/c mice were inoculated with 0.5×10^6 CT26 cells s.c. on the right side of their abdomen, tumor growth was monitored with a digital caliper. Ibrutinib and anti–PD-L1 antibody were IP injected. (*C*) Tumor growth curves (n = 10 mice per group): nontreated: ibrutinib, not significant; nontreated:anti–PD-L1, $P = 0.038$; nontreated:ibrutinib and anti–PD-L1, $P = 0.002$. Pictures demonstrating tumor growth were taken on day 7 posttreatment. (*D*) Intracellular IFN-γ production of CD8+ cells (n = 6 mice per group). On day 7 posttreatment, splenocytes were cocultured with either media or 1×10^6 irradiated 4T1 or CT26 cells for 24 h and in the presence of monensin for the last 6 h. Intracellular IFN-γ were assayed and results were gated on CD3+ cells. Indicated are the proportion of IFN-γ+ cells as a percentage of CD44hi cells. (*E*) On day 7 posttreatment, mice bone marrows were stained for tetramer. (*Left*) Control (influenza nuclear protein). (*Right*) AH1 tetramer. Results were gated on CD8 cells; indicated are the percentages of CD8+tet+ cells (n = 4 mice per group). (*F*) Kaplan–Meier survival plots of the treated mice (n = 10 mice per group). (*G*) Percentage of IFN-γ+ cells of splenocytes incubated with Media, irradiated CT26 or 4T1-Luc cells. (*H*) Percentage of CD8+AH1tet+ cells in bone marrow of treated mice.

augmenting a T-cell immune response. Using the A20 lymphoma and J558 myeloma models, we demonstrated that ibrutinib in combination with anti–PD-L1 induced an antitumor immune response that could cure mice bearing established tumors. These tumors express the BTK enzyme but are insensitive to direct effects of ibrutinib, hence, BTK expression does not guarantee sensitivity to ibrutinib. By combining ibrutinib and anti–PD-L1 antibody we were able to target the host with both agents rather than targeting the tumor. Next, we chose two solid tumors that do not even express BTK: 4T1-breast cancer and CT26-colon cancer. Likewise in both of these models, the combination of ibrutinib with anti–PD-L1 significantly delayed tumor growth and improved survival relative to either therapy alone.

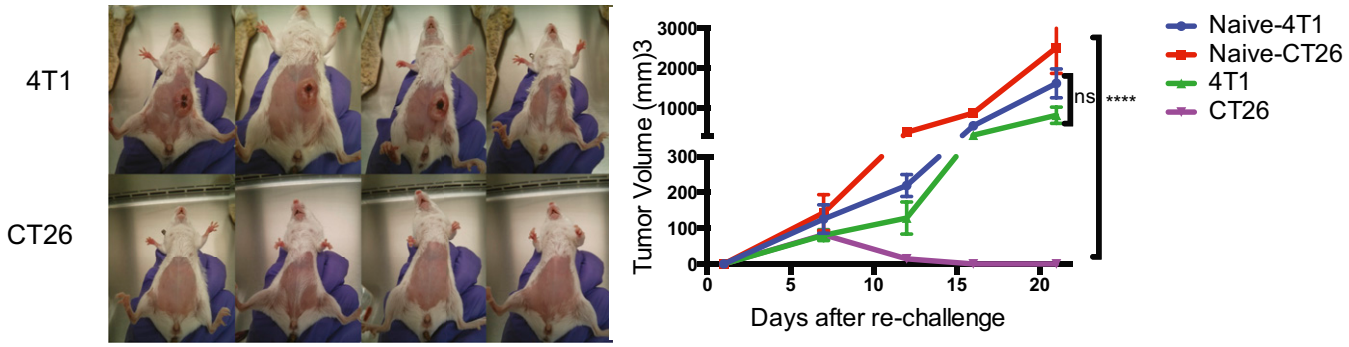

Fig. 5. The combination of ibrutinib and anti–PD-L1 resulted in a long-term antitumor memory of the cured animals. Mice cured from C26 colon cancer were rechallenged s.c. 90 d later in the left side of their abdomen with 1×10^6 CT26 ($n = 4$ mice per group) or 20,000 4T1-Luc cells ($n = 4$ mice per group). As a control, naïve mice were also inoculated with the same cells ($n = 8$ mice per group). (*Left*) Tumor growth following 4T1-Luc or CT26 cell inoculation. Pictures were taken on day 17 post rechallenge. (*Right*) Tumor growth curve following the rechallenge; error bars indicate SEM $P < 0.0001$.

The primary target of ibrutinib is Bruton's tyrosine kinase, a member of the TEC tyrosine kinase family. Previous research (19) showed that ibrutinib, among other kinases, targets ITK, an enzyme required by Th2 T cells, allowing a shift of T-cell immune responses to a Th1 T bias. We therefore hypothesized that ibrutinib could sculpt the antitumor T-cell immune response mediated by PD1/PD-L1 blockade and augment the effectiveness of that response. In both the A20 and CT26 mouse models, anti–PD-L1 treatment alone resulted in some therapeutic effect. By depleting T cells during this therapy we confirmed that these antitumor responses were T-cell mediated. However, we were unable to detect tumor specific T cells in the spleens of these mice. This discrepancy is likely due to the limited sensitivity of the in vitro IFN-γ response assay. In contrast, we were able to demonstrate tumor-specific T cells by this same assay in the spleens of all mouse models treated with the combination of anti–PD-L1 and ibrutinib. Moreover, the responding T cells in these assays were of the memory CD8 T-cell subset.

Response to PD1/PD-L1 blockade is more likely when the tumor or other cells in the tumor microenvironment express PD-L1 (10). Both the 4T1 and CT26 cell lines express very low levels of PD-L1 and both responded to the anti–PD-L1 ibrutinib combination. This result suggests that pretreatment PD-L1 levels do not necessarily predict a response to the combination treatment.

Because the CT26 tumor expresses a known antigen for which there is an MHC-tetramer (17), we were able to detect T cells in mice cured by the combined therapy that recognize this specific tumor antigen. Clearly, this antigen is only one among many against which the antitumor immune response is directed in these cured mice. Mice cured of CT26 tumors by the combination of ibrutinib and anti–PD-L1 displayed long-term memory because they rejected CT26 tumors upon rechallenge. This memory was specific for the antigens of the CT26 tumor as opposed to those contained within the 4T1 breast cancer of the same mouse strain.

The 4T1 mouse mammary tumor cell line is one of the few breast cancer models with the capacity to metastasize efficiently to the lungs, liver brain and bones (22, 23) sites reflective of human breast cancer. MDSCs are massively increased in the blood of animals bearing the 4T1 tumor. MDSCs are known to express PD-L1 and to mediate T-cell suppression (24), thereby allowing tumor metastasis to develop (24). In our experiments, MDSCs from blood of tumor bearing mice expressed low levels of PD-L1 (Fig. S8) and the number of peripheral blood and splenic MDSCs did not change following the combined ibrutinib and anti–PD-L1 treatment (Fig. S7). Other studies have reported that anti–PD-L1 treatment alone is insufficient to alter MDSC arginase activity, expression of Nos-2 or NO production (25). Only by combining anti–PD-L1 with anti-CTLA4 mAb and two epigenetic-modulating drugs were MDSC's numbers reduced (26). Our results suggest that the antitumor effect of the combination of ibrutinib and anti–PD-L1 is not mediated through MDSCs, but rather through the direct activation of T cells.

We observed diversity in the response to anti–PD-L1 treatment within genetically identical BALB/c mice. There were subgroups of responders and nonresponders. This variability, reminiscent of what has been observed in patients treated by PD-1/PD-L1 blockade, may perhaps be explained by the variable immunologic histories of the individual mice, resulting in differences of their T-cell receptor (TCR) repertoire. The addition of ibrutinib to anti–PD-L1 treatment increased the proportion of mice in the responding subgroup. We performed all experiments at least three times. Variability was seen in the magnitude of the effect; however, the results consistently showed smaller tumor size and improved survival with the combination of ibrutinib and anti–PD-L1 antibody.

As new immune and targeted therapies become available, there is an urgent need to find additive and synergistic combinations of these agents. Occasionally such combinations will be antagonistic rather than additive or synergistic. The primary target of ibrutinib is thought to be BTK and therefore it has been initially developed as a treatment for B-cell malignancies. However, it may also have a role to play as an enhancer of T-cell therapies. By virtue of its other targets in T cells, ibrutinib may be a promising candidate to combine with T-cell modulating therapies.

Antibodies against both PD-L1 and PD-1 are effective at restoring antitumor immune function in human cancers. Antibodies targeting PD-L1 do not block PD-L2 a second ligand of PD-1. It remains an open question how these two blocking strategies would compare as single agents and in combinations.

The combinatorial effect demonstrated here argues for a clinical evaluation of ibrutinib as an enhancer of the antitumor therapeutic effects of PD-1 blockade in both ibrutinib-resistant lymphomas and in other cancers that do not even express BTK.

Materials and Methods

Reagents. Ibrutinib was provided by Pharmacyclics. Anti-mouse PD-L1, Clone 10F.9G2, antibody was purchased from BioXcell. The isotype control rat hybridoma, SFR8-B6 (ATCC HB-152) was produced as ascites in SCID mice by Bionexus.

The following monoclonal antibodies (mAbs) were used for flow cytometry: rat anti-mouse CD4-PerCP cy5.5, rat anti-mouse CD3-PerCP cy5.5, rat anti-mouse CD8a-FITC, rat anti-mouse CD44-APC, rat anti-mouse CD49b-APC, rat anti-mouse IFN-gamma-PE, hamster anti-mouse CD80-PE. These antibodies and their isotype controls were purchased from either BD Biosciences or eBioscience.

Cell Lines and Mice. A20, a B-cell lymphoma line, and CT26 colon carcinoma line were obtained from ATCC; 4T1-Luc breast carcinoma cell line was a gift

from the S. Strober laboratory and the C. Contag laboratory (both at Stanford University). The H11 pre–B-cell line was generated from a C57BL/6 mouse as described (27) 2F3-leukemia cell line was generated from a BALB/c mouse as described (28). Tumor cells were cultured in complete medium (RPMI 1640; Cellgro) containing 10% (vol/vol) FBS (HyClone), 100 U/mL penicillin, 100 μg/mL streptomycin, and 50 μM 2-ME (Gibco).

Six- to 8-week-old female BALB/c were purchased from JAX Laboratories or Charles River. Mice were housed in the Laboratory Animal Facility of the Stanford University Medical Center (Stanford, CA). All experiments were approved by the Stanford Administrative Panel on Laboratory Animal Care and conducted in accordance with Stanford University Animal Facility and National Institutes of Health guidelines.

Tumor Inoculation and Animal Studies. A20 cells (5×10^6) were injected s.c. at sites on both right and left abdomen. 4T1-luc and CT26 tumor cells (0.01×10^6 and 0.5×10^6, respectively) were injected to the right side of the abdomen.

Ibrutinib was injected by the i.p. route at a dose of 6 mg/kg beginning on day 8 after tumor implantation or when tumors reached a minimal size of 5mm in the largest diameter and continued daily for 8–14 d.

Tumor size were monitored with a digital caliper (Mitutoyo) every 2–3 d and expressed as volume (length × width × height). Mice were killed when tumor size reached 1.5 cm in the largest diameter when inoculated with 2 tumors and 2 cm when inoculated with one as per guidelines.

4T1-Luc tumor challenged mice were analyzed for lung metastasis by injecting India ink through the trachea. Lungs were then excised, washed once in water and fixed in Fekete's solution (100 mL of 70% alcohol, 10 mL of formalin, and 5 mL of glacial acetic acid) at room temperature. Surface metastases subsequently appeared as white nodules at the surface of black lungs and were counted under a microscope. For bioluminescence assessment, mice were anesthetized with isoflurane gas (2% isoflurane in oxygen, 1 L/min). d-Luciferin (Biosynth AG) was i.p. injected at a dose of 150 mg/kg (saturating substrate concentration for luciferase enzyme). Mice were imaged in a light-tight chamber using an in vivo optical imaging system (IVIS 100; Xenogen) equipped with a cooled charge-coupled device camera. During image recording, mice inhaled isofluorane delivered via a nose cone, and their body temperature was maintained at 37 °C in the dark box of the camera system. Bioluminescence images were acquired between 10 and 20 min after luciferin administration. Mice usually recovered from anesthesia within 2 min after imaging.

Depletion of CD4 and CD8 T Cells. Anti-CD4 (GK1.5 clone- rat IgG2b) and anti-CD8 (2.43 clone- rat IgG2b) mAbs (BioXcell) were injected 2 d and 1 d before therapy, on the day therapy was begun, and at 5 and 8 d after beginning of therapy, at a dose of 0.5 or 0.1 mg per injection for CD4 and CD8, respectively. The depletion conditions were validated by flow cytometry of blood showing specific depletion of more than 95% of each respective cell subset.

Flow Cytometry. Cells were surface stained in PBS, 1% FBS, and 0.01% sodium azide, fixed in 2% (wt/vol) paraformaldehyde, and analyzed by flow cytometry on an FACSCalibur (BD Biosciences). Data were stored and analyzed using Cytobank (www.cytobank.org/).

Statistical Analysis. Prism software (GraphPad) was used to analyze tumor growth and to determine statistical significance of differences between groups by applying an unpaired Student's *t* test. P values < 0.05 were considered significant.

In Vitro Assays. Growth and viability of cells was measured using Prestoblue Cell Viability reagent (Life Technologies) according to the manufacturer's protocol.

IFNγ Assay. Single cell suspensions were made from spleens of treated mice, red cells were lysed with ammonium chloride, potassium buffer (Quality Biological). Splenocytes were then cocultured with 1×10^6 irradiated CT26, 4T1-luc, or A20 cells for 24 h at 37 °C and 5% CO_2 in the presence of 0.5 μg of anti-mouse CD28mAb (BD PharMingen). Monensin (Golgistop; BD Biosciences) was added for the last 5 h. Intracellular IFNγ expression was assessed using BD Cytofix/Cytoperm Plus kit per manufacturers instructions.

Tetramer Staining. PE-conjugated H-2Ld tetramer to peptide SPSYVYHQF (MuLV env gp70 423–431) was purchased from Proimmune; PE-conjugated H-2Ld tetramer to peptide IASNENMETMESSTLE (influenza nucleoprotein 365–380) was a gift from The M. Davis lab (Stanford University). Antibodies were used at 5 μg/mL, and surface staining was performed in FACS buffer on ice for 30 min.

ACKNOWLEDGMENTS. The authors gratefully acknowledge Principia biopharma for the occupancy studies, Prof. Mark Davis and Dr. Evan Newelll for the control tetramer. This work was supported by Boaz and Varda Dotan, the National Institute of Health Grant (P01 CA034233), and by Pharmacyclics.

1. Korman AJ, Peggs KS, Allison JP (2006) Checkpoint blockade in cancer immunotherapy. *Adv Immunol* 90:297–339.
2. Sondak VK, Smalley KS, Kudchadkar R, Grippon S, Kirkpatrick P (2011) Ipilimumab. *Nat Rev Drug Discov* 10(6):411–412.
3. Poole RM (2014) Pembrolizumab: First global approval. *Drugs* 74(16):1973–1981.
4. Keir ME, Butte MJ, Freeman GJ, Sharpe AH (2008) PD-1 and its ligands in tolerance and immunity. *Annu Rev Immunol* 26:677–704.
5. Ohigashi Y, et al. (2005) Clinical significance of programmed death-1 ligand-1 and programmed death-1 ligand-2 expression in human esophageal cancer. *Clin Cancer Res* 11(8):2947–2953.
6. Konishi J, et al. (2004) B7-H1 expression on non-small cell lung cancer cells and its relationship with tumor-infiltrating lymphocytes and their PD-1 expression. *Clin Cancer Res* 10(15):5094–5100.
7. Thompson RH, et al. (2006) Tumor B7-H1 is associated with poor prognosis in renal cell carcinoma patients with long-term follow-up. *Cancer Res* 66(7):3381–3385.
8. Thompson RH, et al. (2004) Costimulatory B7-H1 in renal cell carcinoma patients: Indicator of tumor aggressiveness and potential therapeutic target. *Proc Natl Acad Sci USA* 101(49):17174–17179.
9. Brahmer JR, et al. (2012) Safety and activity of anti-PD-L1 antibody in patients with advanced cancer. *N Engl J Med* 366(26):2455–2465.
10. Topalian SL, et al. (2012) Safety, activity, and immune correlates of anti-PD-1 antibody in cancer. *N Engl J Med* 366(26):2443–2454.
11. Hamid O, et al. (2013) Safety and tumor responses with lambrolizumab (anti-PD-1) in melanoma. *N Engl J Med* 369(2):134–144.
12. Ansell SM, et al. (2014) PD-1 blockade with Nivolumab in relapsed or refractory Hodgkin's lymphoma. *N Engl J Med* 372(4):311–319.
13. Wolchok JD, et al. (2013) Nivolumab plus ipilimumab in advanced melanoma. *N Engl J Med* 369(2):122–133.
14. Zamarin D, et al. (2014) Localized oncolytic virotherapy overcomes systemic tumor resistance to immune checkpoint blockade immunotherapy. *Sci Transl Med* 6(226):226ra32.
15. Cooper ZA, et al. (2014) Response to BRAF inhibition in melanoma is enhanced when combined with immune checkpoint blockade. *Cancer Immunol Res* 2(7):643–654.
16. Honigberg LA, et al. (2010) The Bruton tyrosine kinase inhibitor PCI-32765 blocks B-cell activation and is efficacious in models of autoimmune disease and B-cell malignancy. *Proc Natl Acad Sci USA* 107(29):13075–13080.
17. Advani RH, et al. (2013) Bruton tyrosine kinase inhibitor ibrutinib (PCI-32765) has significant activity in patients with relapsed/refractory B-cell malignancies. *J Clin Oncol* 31(1):88–94.
18. Barrientos J, Rai K (2013) Ibrutinib: A novel Bruton's tyrosine kinase inhibitor with outstanding responses in patients with chronic lymphocytic leukemia. *Leuk Lymphoma* 54(8):1817–1820.
19. Dubovsky JA, et al. (2013) Ibrutinib is an irreversible molecular inhibitor of ITK driving a Th1-selective pressure in T lymphocytes. *Blood* 122(15):2539–2549.
20. Huang AY, et al. (1996) The immunodominant major histocompatibility complex class I-restricted antigen of a murine colon tumor derives from an endogenous retroviral gene product. *Proc Natl Acad Sci USA* 93(18):9730–9735.
21. Ribas A, Hodi FS, Callahan M, Konto C, Wolchok J (2013) Hepatotoxicity with combination of vemurafenib and ipilimumab. *N Engl J Med* 368(14):1365–1366.
22. Lelekakis M, et al. (1999) A novel orthotopic model of breast cancer metastasis to bone. *Clin Exp Metastasis* 17(2):163–170.
23. Pulaski BA, Ostrand-Rosenberg S (2001) Mouse 4T1 breast tumor model. *Curr Prot Immunol* 20:20.2.
24. Youn JI, Nagaraj S, Collazo M, Gabrilovich DI (2008) Subsets of myeloid-derived suppressor cells in tumor-bearing mice. *J Immunol* 181(8):5791–5802.
25. Noman MZ, et al. (2014) PD-L1 is a novel direct target of HIF-1α, and its blockade under hypoxia enhanced MDSC-mediated T cell activation. *J Exp Med* 211(5):781–790.
26. Kim K, et al. (2014) Eradication of metastatic mouse cancers resistant to immune checkpoint blockade by suppression of myeloid-derived cells. *Proc Natl Acad Sci USA* 111(32):11774–11779.
27. Li J, et al. (2007) Lymphoma immunotherapy with CpG oligodeoxynucleotides requires TLR9 either in the host or in the tumor itself. *J Immunol* 179(4):2493–2500.
28. Shoham T, Rajapaksa R, Kuo CC, Haimovich J, Levy S (2006) Building of the tetraspanin web: Distinct structural domains of CD81 function in different cellular compartments. *Mol Cell Biol* 26(4):1373–1385.